Quantum phase flip gate based on plasmonic double-bar resonators

Xing Ri Jin and Jie Gao*

Department of Mechanical and Aerospace Engineering, Missouri University of Science and Technology, Rolla, Missouri 65409, USA
**Corresponding author: gaojie@mst.edu*

Received April 10, 2013; accepted May 10, 2013;
posted May 20, 2013 (Doc. ID 188554); published June 11, 2013

We demonstrate a quantum phase flip gate between two QDs that resonantly couple to plasmonic double-bar resonators with asymmetric coupling strengths. Large coupling strengths can be achieved due to the deep subwavelength mode volumes of the optical modes in plasmonic double-bar resonators. High fidelity (~98%) and high success probability of the phase gate operation have been obtained when the coupling strength ratio (g_2/g_1) and resonant mode decay rate (κ/g_1) are optimized. The subwavelength-scale plasmonic structures provide tremendous potential for solid-state quantum information processing. © 2013 Optical Society of America

OCIS codes: (250.5403) Plasmonics; (230.5590) Quantum-well, -wire and -dot devices; (270.5580) Quantum electrodynamics; (270.5585) Quantum information and processing.
http://dx.doi.org/10.1364/OL.38.002110

Surface plasmons, which are collective excitations of electrons at the metal–dielectric interface [1], play very important roles in confining electromagnetic wave in the deep subwavelength scale for realizing functional nanophotonic devices and integrated systems. Surface plasmons reveal strong analogies to light propagation in conventional dielectric optical components and have many promising applications in quantum computation and quantum information processing. The scattering properties of surface plasmons interacting with quantum dots (QDs) in plasmonic waveguides have been widely studied [2,3]. One-dimensional plasmonic waveguides with deep subwavelength confinement enable remarkable nonlinearity to implement a single-photon transistor [4]. When plasmonic nanocavities are introduced, such as plasmonic microdisk resonators [5], metallic-fin Fabry–Pérot cavities [6], and hybrid photonic–plasmonic crystal nanocavities [7], high quality factor to mode volume ratios provide extremely large coupling strengths between quantum emitters and the resonant modes. Recently, several schemes for two-qubit entanglement mediated by plasmonic waveguides [8–11] and nanoring resonators [12] have been reported. A quantum phase gate of QDs coupled with highly detuned plasmon modes in a metallic nanoring resonator has also been proposed [13], where classical laser pulses from nanotips are utilized in order to obtain a high-fidelity phase gate.

In this Letter, we investigate a scheme for realizing the quantum phase flip gate between two QDs that are resonantly coupled to a plasmonic double-bar resonator with asymmetric coupling strengths. The quadrupole resonant mode in the double-bar resonator has a deep subwavelength mode volume. As a result, very large coupling strengths between QDs and the resonant mode can be achieved and can be even greater than the decay rates of QDs and the resonant mode at low temperature. The dependence of phase gate fidelity and success probability on QD-resonator coupling strengths and the decay rate of plasmonic resonant mode are systematically discussed. Most important, practical parameters are considered here to investigate the performance of a realistic compact quantum phase flip gate.

The proposed system is composed of two identical three-level QDs [14,15] located along the center line of a double-bar resonator in the x direction on a glass substrate, as shown in Fig. 1(a). Two silver bars forming the resonator have the geometries of 220 nm in length, 60 nm in width, with a gap of 30 nm and silver thickness of 15 nm. The permittivity of silver is described by the Drude model with plasmon frequency ω_p of 1.366×10^{16} rad/s and collision frequency γ of 4.2×10^{13} rad/s at room temperature of 300 K [16]. The refractive index of the glass substrate is 1.5. The double-bar resonator supports the quadrupole-like plasmonic resonant mode at the frequency ω_{pl} of 206 THz [as depicted in the spectrum of Fig. 1(b)] with the electric field intensity distribution shown in Fig. 1(c). The QDs have one excited state $|e\rangle$ and two ground states $|g\rangle$ and $|f\rangle$, and the transition between states $|e\rangle$ and $|g\rangle$ is coupled to the quadrupole-like resonant mode. State $|f\rangle$ is largely detuned and not involved in the interaction with the resonant mode.

When two QDs simultaneously interact with the double-bar plasmonic mode on resonance with coupling

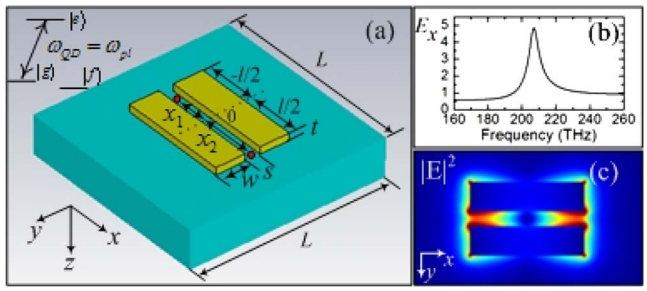

Fig. 1. (a) Schematic of the proposed structure consisting of a silver double-bar resonator and two QDs on a glass substrate. The resonator geometric parameters are thickness $t = 15$ nm, length $l = 220$ nm, width $w = 60$ nm, and gap $s = 30$ nm. The positions of two QDs are represented by x_1 and x_2, respectively. The unit cell with $L = 900$ nm can be repeated to form periodic arrays. The top left inset shows the energy diagram of a three-level QD, where the transition between $|e\rangle$ and $|g\rangle$ couples to the plasmonic resonant mode. (b) and (c) show the spectral response of the quadrupole-like mode supported in the double-bar resonator and the electric field intensity $|E|^2$ distribution.

 © 2013 Optical Society of America

strengths g_1 and g_2, the effective Hamiltonian can be written as (assuming $\hbar = 1$ and $\omega_{QD} = \omega_{pl}$)

$$H_{eff} = g_1(a^\dagger S_1^- + aS_1^+) + g_2(a^\dagger S_2^- + aS_2^+) - i\frac{\kappa}{2}a^\dagger a - i\frac{\Gamma}{2}\sum_{j=1}^{2}|e\rangle_j\langle e_j|, \quad (1)$$

where $a^\dagger$ and a are the creation and annihilation operators for the plasmonic resonant mode. $S_j^- = |g\rangle_j\langle e_j|$ and $S_j^+ = |e\rangle_j\langle g_j|(j = 1, 2)$ are the lowering and raising operators for the jth QD, respectively. κ is the decay rate of the resonant mode, Γ is the decay rate of QDs, and $g_j(j = 1, 2)$ is the coupling strength between the resonant mode and the jth QD.

The QD-resonator coupling strength is given by $g = \mu\sqrt{(\omega/2\varepsilon\hbar V_{mode})}|(E/E_{max})|$ [17], where μ is the QD dipole moment and V_{mode} is the mode volume of the double-bar resonant mode. Typically, μ is of the order of 10^{-28} C m for semiconductor QDs [18,19]. The mode volume V_{mode} is 1.48×10^{-23} m^3 based on the finite-element-method simulation. Therefore, a coupling strength g_{max} of ~21.6 THz can be achieved when the QD is positioned at the maximum of the electric field intensity. At the same time, different coupling strengths g can be realized by manipulating QD positions, since coupling strength is proportional to the electric field intensity where the QD is located. The quality factor (Q) of the resonant mode is 35 based on finite-difference time-domain simulation, resulting in a mode decay rate $\kappa = \omega/(2Q) \sim$ 18.63 THz at room temperature (300 K). However, at low temperature, the collision frequency γ of silver is scaled down by a ratio of the electrical conductivity at low temperature and room temperature [16,20,21]. Figure 2 shows that the Q factors (red triangles) of the resonant mode increase from 35 to 296 when temperature is decreased from 300 to 10 K. Within the same temperature range, the decay rate κ/g_1 (blue squares) can be reduced from 1.660 to 0.194 when we choose $g_1 = g_2/\sqrt{3}$, $g_2 = 0.9g_{max}$ under practical considerations. The QD decay rate Γ, including the spontaneous emission decay and the dephasing, also varies with temperature, and we choose $\Gamma = \kappa$ for convenience without loss of generality.

The quantum phase gate can be constructed by assuming that the quantum information is encoded in a subspace spanned by the QD states $\{|e_1\rangle, |g_1\rangle, |g_2\rangle, |f_2\rangle\}$. Based on the effective Hamiltonian in Eq. (1), after an interaction time t, the evolutions of the QDs and plasmonic resonant mode are

$$\begin{aligned}
&|g_1\rangle|g_2\rangle|0\rangle \to |g_1\rangle|g_2\rangle|0\rangle, |g_1\rangle|f_2\rangle|0\rangle \to |g_1\rangle|f_2\rangle|0\rangle,\\
&|e_1\rangle|g_2\rangle|0\rangle \to a|e_1\rangle|g_2\rangle|0\rangle + b|g_1\rangle|e_2\rangle|0\rangle + c|g_1\rangle|g_2\rangle|1\rangle,\\
&|e_1\rangle|f_2\rangle|0\rangle \to a_1|e_1\rangle|f_2\rangle|0\rangle + b_1|g_1\rangle|f_2\rangle|1\rangle, \quad (2)
\end{aligned}$$

where

$$\begin{aligned}
a &= \frac{1}{g_1^2+g_2^2}\left[g_1^2 e^{-\frac{(\kappa+\Gamma)t}{4}}(\cos(\Delta t) + \frac{\kappa-\Gamma}{4\Delta}\sin(\Delta t)) + g_2^2 e^{-\Gamma t/2}\right],\\
b &= \frac{g_1 g_2}{g_1^2+g_2^2}\left[e^{-\frac{(\kappa+\Gamma)t}{4}}(\cos(\Delta t) + \frac{\kappa-\Gamma}{4\Delta}\sin(\Delta t)) - e^{-\Gamma t/2}\right],\\
c &= -i\frac{g_1}{\Delta}e^{-\frac{(\kappa+\Gamma)t}{4}}\sin(\Delta t),\\
a_1 &= e^{-\frac{(\kappa+\Gamma)t}{4}}\left[\cos(\delta t) + \frac{\kappa-\Gamma}{4\delta}\sin(\delta t)\right],\\
b_1 &= -i\frac{g_1}{\delta}e^{-\frac{(\kappa+\Gamma)t}{4}}\sin(\delta t),\\
\Delta &= \sqrt{g_1^2+g_2^2-\left(\frac{\kappa-\Gamma}{4}\right)^2}, \quad \text{and} \quad \delta = \sqrt{g_1^2-\left(\frac{\kappa-\Gamma}{4}\right)^2}.
\end{aligned} \quad (3)$$

If the interaction time satisfies $g_1 t = \pi$, $g_2/g_1 = \sqrt{3}$, and $\Gamma = \kappa \ll g_1$, we could obtain a near-perfect two-qubit phase gate,

$$\begin{aligned}
&|g_1\rangle|g_2\rangle|0\rangle \to |g_1\rangle|g_2\rangle|0\rangle, \quad |g_1\rangle|f_2\rangle|0\rangle \to |g_1\rangle|f_2\rangle|0\rangle,\\
&|e_1\rangle|g_2\rangle|0\rangle \to |e_1\rangle|g_2\rangle|0\rangle, \quad |e_1\rangle|f_2\rangle|0\rangle \to -|e_1\rangle|f_2\rangle|0\rangle. \quad (4)
\end{aligned}$$

Achieving high gate fidelity and a high success probability with practical parameters is essential for a quantum phase flip gate. According to Eq. (2), the fidelity F can be examined by $(1/4)(1/(2 + |a|^2 + |a_1|^2))(2 + |a| + |a_1|)^2$, and the success probability P is described by $(1/4)(2 + |a|^2 + |a_1|^2)$, with respect to the initial state $|\psi_0\rangle = (1/2)(|e_1\rangle + |g_1\rangle)(|g_2\rangle + |f_2\rangle)$. Figure 3(a) shows the fidelity as a function of coupling strength ratio g_2/g_1 and time $g_1 t$ with $\kappa = \Gamma = 0.1g_1$. Clearly, the fidelity F experiences a damped oscillation over time, and the maximum value is obtained when time $g_1 t$ is chosen to be around π. Also, asymmetric coupling strengths $g_2/g_1 >$ 1.3 are allowed for fidelity to be maintained above 0.95. On the other hand, the fidelity F decreases when decay rate κ/g_1 is increased, as shown in Fig. 3(b) when $g_1 t = \pi$ and $\kappa = \Gamma$. This indicates that large coupling strengths will enable high-fidelity phase gate operation, and the fidelity F can reach above 0.95 when $\kappa/g_1 < 0.2$. Similarly, the success probability P of the gate operation is examined as a function of coupling strength ratio g_2/g_1, time $g_1 t$, and decay rate κ/g_1 in Figs. 4(a) and 4(b). The high success probability is obtained when $g_2/g_1 > 1.3$, $g_1 t = \pi$, and $\kappa/g_1 < 0.2$. Therefore, a large coupling strength $g_1 > 5\kappa$ is necessary in order to get both high fidelity and high success probability within a short gate time. From the analysis of the designed plasmonic double-bar resonators coupled with two QDs, it is

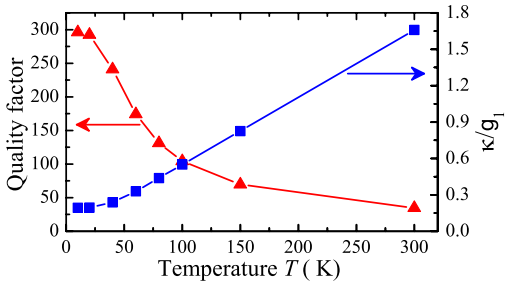

Fig. 2. Dependence of the plasmonic resonant mode Q factor (red triangles) and the decay rate κ/g_1 (blue squares) on temperature T.

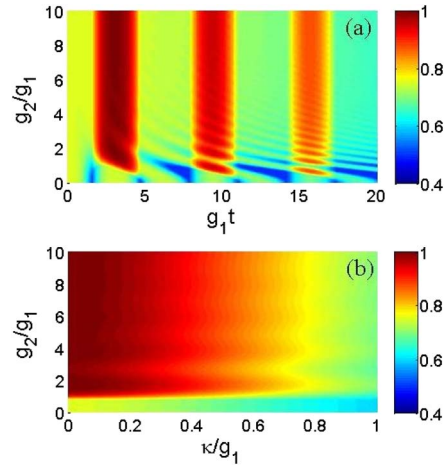

Fig. 3. (a) Fidelity F as a function of coupling strength ratio g_2/g_1 and time g_1t with $\kappa = \Gamma = 0.1g_1$. (b) Fidelity F as a function of coupling strength ratio g_2/g_1 and decay rate κ/g_1 when $g_1t = \pi$ and $\kappa = \Gamma$.

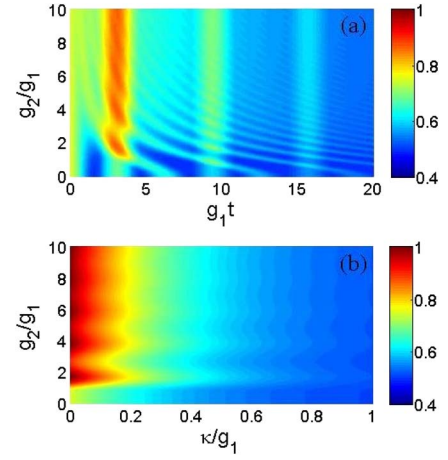

Fig. 4. (a) Success probability P as a function of coupling strength ratio g_2/g_1 and time g_1t with $\kappa = \Gamma = 0.1g_1$. (b) Success probability P as a function of coupling strength ratio g_2/g_1 and decay rate κ/g_1 when $g_1t = \pi$ and $\kappa = \Gamma$.

feasible to achieve $g_2 = 0.9g_{\max}$, $g_2/g_1 = \sqrt{3}$, and $\kappa/g_1 = 0.194$, which leads to high fidelity ~0.98 and success probability ~0.77 for the quantum phase flip gate operation.

In conclusion, a realistic scheme for a quantum phase flip gate between two QDs resonantly coupled to a plamsonic double-bar resonator has been proposed and demonstrated with practical parameters. Because of the ultrasmall mode volume of the double-bar resonant mode, high fidelity ~0.98 and a high success probability can be achieved when the QDs couple to the resonant mode with asymmetric coupling strengths at low temperature. This compact device can be easily fabricated by using standard nanofabrication procedures [22]. Furthermore, the double-bar resonators can be periodically arranged on a glass substrate to form a two-qubit phase gate array. All of these advantages show that the QD-plasmonic resonator system is very promising to implement solid-state quantum information processing with subwavelength footprints.

The authors thank Q. Wang and X. Yang for very helpful discussions. This work was supported by the Department of Mechanical and Aerospace Engineering at Missouri S&T and the University of Missouri Research Board.

References

1. H. Raether, *Surface Plasmons* (Springer, 1988).
2. A. V. Akimov, A. Mukherjee, C. L. Lu, D. E. Chang, A. S. Zibrov, P. R. Hemmer, H. Park, and M. D. Lukin, Nature **450**, 402 (2007).
3. M. T. Cheng and Y. Y. Song, Opt. Lett. **37**, 978 (2012).
4. D. E. Chang, A. S. Sørensen, E. A. Demler, and M. D. Lukin, Nat. Phys. **3**, 807 (2007).
5. B. Min, E. Ostby, V. Sorger, E. Ulin-Avila, L. Yang, X. Zhang, and K. Vahala, Nature **457**, 455 (2009).
6. V. J. Sorger, R. F. Oulton, J. Yao, G. Bartal, and X. Zhang, Nano Lett. **9**, 3489 (2009).
7. X. Yang, A. Ishikawa, X. Yin, and X. Zhang, ACS Nano **5**, 2831 (2011).
8. G. Y. Chen and Y. N. Chen, Opt. Lett. **37**, 4023 (2012).
9. A. Gonzalez-Tudela, D. Martin-Cano, E. Moreno, L. Martin-Moreno, C. Tejedor, and F. J. Garcia-Vidal, Phys. Rev. Lett. **106**, 020501 (2011).
10. D. Martin-Cano, A. Gonzalez-Tudela, L. Martin-Moreno, F. J. Garcia-Vidal, C. Tejedor, and E. Moreno, Phys. Rev. B **84**, 235306 (2011).
11. G. Y. Chen, N. Lambert, C. H. Chou, Y. N. Chen, and F. Nori, Phys. Rev. B **84**, 045310 (2011).
12. G. Y. Chen, C. M. Li, and Y. N. Chen, Opt. Lett. **37**, 1337 (2012).
13. Z. R. Lin, G. P. Guo, T. Tu, H. O. Li, C. L. Zou, J. X. Chen, Y. H. Lu, X. F. Ren, and G. C. Guo, Phys. Rev. B **82**, 241401 (2010).
14. M. Califano, A. Franceschetti, and A. Zunger, Nano Lett. **5**, 2360 (2005).
15. M. Atatüre, J. Dreiser, A. Badolato, A. Högele, K. Karrai, and A. Imamoglu, Science **312**, 551 (2006).
16. M. K. Seo, S. H. Kwon, H. S. Ee, and H. G. Park, Nano Lett. **9**, 4078 (2009).
17. Y. Gong and J. Vučković, Appl. Phys. Lett. **90**, 033113 (2007).
18. P. G. Eliseez, H. Li, A. Stintz, G. T. Liu, T. C. Newell, K. J. Malloy, and L. F. Lester, Appl. Phys. Lett. **77**, 262 (2000).
19. V. L. Colvin, K. L. Cunningham, and A. P. Alivisatos, J. Chem. Phys. **101**, 7122 (1994).
20. S. H. Kwon, J. H. Kang, C. Seassal, S. K. Kim, P. Regreny, Y. H. Lee, C. M. Lieber, and H. G. Park, Nano Lett. **10**, 3679 (2010).
21. D. R. Lide, *Handbook of Chemistry and Physics*, 90th ed. (CRC Press, 2009).
22. N. Liu, L. Langguth, T. Weiss, J. Kästel, M. Fleischhauer, T. Pfau, and H. Giessen, Nat. Mater. **8**, 758 (2009).